

# $^{60}\text{Co}$ $\gamma$ -ray irradiation effects on the interface traps density of tin oxide films of different thicknesses on n-type Si (111) substrates

N. Tuğluoğlu \*

Department of Nuclear Electronics and Instrumentation, Sarayköy Nuclear Research and Training Center, 06983, Saray, Ankara, Turkey

Received 25 September 2006; received in revised form 27 October 2006

Available online 11 December 2006

## Abstract

We report the first investigation of the gamma irradiation effects on interface state density and series resistance determined from capacitance–voltage ( $C$ – $V$ ) and conductance–voltage ( $G$ – $V$ ) characteristics in  $\text{Au}/\text{SnO}_2/\text{n-Si}$  (MOS) structures prepared at various  $\text{SnO}_2$  layer thicknesses by spray deposition technique. It was fabricated three samples depending on deposition time. The samples were irradiated using a  $^{60}\text{Co}$   $\gamma$ -ray source irradiation with the total dose range was 0–500 kGy at room temperature. The  $C$ – $V$  and  $G$ – $V$  measurements of the samples were performed at high frequency (500 kHz) at room temperature before and after irradiation. The measurement capacitance and conductance are corrected for series resistance. The thicknesses of  $\text{SnO}_2$  films obtained from the measurement of the oxide capacitance in the accumulation region for MOS Schottky diodes were 19, 52, 191 Å, for D1, D2 and D3 samples, respectively. It has been seen that the value of the series resistance  $R_s$  of samples D1 (50  $\Omega$ ), D2 (66  $\Omega$ ) and D3 (157  $\Omega$ ) increases with increasing the oxide layer thickness and increases from 50  $\Omega$  to 62.7  $\Omega$  with increasing irradiation dose. The single frequency method of Hill-Coleman was used to determine the interface state density ( $D_{it}$ ).

© 2006 Elsevier B.V. All rights reserved.

PACS: 61.80.Ed; 61.80.–x; 73.20.At; 73.40.Qv; 84.37.+q

Keywords: MOS diodes;  $\text{SnO}_2$ ;  $^{60}\text{Co}$   $\gamma$ -ray;  $C$ – $V$ ;  $G$ – $V$ ; Series resistance; Interface state density

## 1. Introduction

$\text{SnO}_2$  thin films have been one of the most important metal oxides due to their properties and potential applications [1–6]. This oxide has been studied and developed for numerous fields of application such as catalysis, electrochemistry, chemical technologies, electronics, metallurgy, biotechnology and nuclear technology [7–10]. There are several deposition techniques used to grow  $\text{SnO}_2$  thin films including rapid oxidation of elemental tin, thermal evaporation of oxide powders, ac–dc magnetron sputtering, sol–gel, chemical vapor deposition, electron beam evaporation, pulsed laser deposition and spray deposition method, each

of which had advantages and disadvantages. Spray deposition method has a simple and inexpensive experimental arrangement and has the advantages like ease of adding doping material, reproducibility, high growth rate, good control of the deposition parameters, low processing temperatures. Deposition of  $\text{SnO}_2$  films by spray deposition method has been studied extensively by several investigators [4–12]. The spray deposition process presents an easy way to integrate  $\text{SnO}_2$  devices into the Si technology.

The metal-semiconductor (MS) contact is one of the most widely used rectifying contacts in device technology [13]. The existence of such an oxide layer ( $\text{SnO}_2$ ) converts the device to a metal-oxide-semiconductor (MOS) diode [5,6,14] and may have a strong influence on the diode characteristics as well as a change of the interface state charge with bias which will give rise to an additional field in the interfacial layer [14]. The series resistance ( $R_s$ ) and interface

\* Tel.: +90 312 815 4300; fax: +90 312 815 4307.

E-mail address: [ntuglu@taek.gov.tr](mailto:ntuglu@taek.gov.tr)

state density ( $D_{it}$ ) of MOS structures are important parameters that affect their main electrical parameters [5,6,14–20]. In the case of  $\text{SnO}_2/\text{Si}$  interface, it is proposed that the structure behaves like a Schottky barrier diode [4–6]. It appears that the  $\text{SnO}_2$  layer plays a more significant role than serving as a contact and is likely to influence the current–voltage characteristics of the  $\text{SnO}_2/\text{Si}$  interface and leads to increase the series resistance of the diodes [5,6]. The existence of an interfacial layer between the metal and the semiconductor play an important role in the determination of the Schottky barrier height and interface state density [5,6]. Various measurement techniques for determining the interface state density have been developed and among them the important one is Hill-Coleman technique [21]. This technique proposed by Hill and Coleman [21] is a powerful tool to deduce interface trap density  $D_{it}$  which is useful in estimating the interface charge and has been used by some authors [22,23].

A number of efforts were devoted to investigate the influence of  $\gamma$ -radiation on the properties of metal oxide materials, e.g.  $\text{In}_2\text{O}_3$ ,  $\text{CeO}_2$ ,  $\text{NiO}$ ,  $\text{TeO}_2$ ,  $\text{SiO}$  [24–29]. It is believed that ionizing radiation causes structural defects (called oxygen vacancies in oxides or colour centers) leading to change in their density on exposure to  $\gamma$ -rays [30,31]. Depending on the electronic structure of the material, the nature of oxygen vacancies changes dramatically [32]. The influence of radiation depends on both the dose and the parameters of the films including their thickness: the degradation is more severe for the higher dose and the thinner films [26,28]. Deep understanding of the physical properties of the materials under the influence of radiation exposure is vital for the effective design of dosimeter devices [29]. Metal-oxide-semiconductor (MOS) structures are extremely sensitive to high-level radiation (e.g. neutrons, ions, electrons and  $\gamma$ -ray) [13–20]. It is well known that the density of interface states between metal and semiconductor interfaces in the metal-semiconductor Schottky structures has been studied more than that in the metal-oxide-semiconductor (MOS) type Schottky structures due to existence of oxide layer between semiconductor and metal that passivates the surface of semiconductor.

The study of interface state density is crucial in order to have a better control on the electrical characteristics of a Schottky junction and to the best of our knowledge, no such report is available for  $^{60}\text{Co}$   $\gamma$ -ray irradiation effects on the interface traps density of tin oxide films of different thicknesses on n-type Si (111) substrates. In this paper, we report the effects of tin oxide film thickness and  $\gamma$ -ray irradiation dose on the series resistance and interface state density of  $\text{Au}/\text{SnO}_2/\text{n-Si}$  (111) Schottky diodes from  $C$ – $V$  and  $G$ – $V$  characteristics. The other purpose of this study was to compare estimates of interface trap densities obtained experimentally dependent on tin oxide film thicknesses for the MOS structures using Hill-Coleman's single frequency technique [21] before and after irradiation.

## 2. Experimental procedure

The metal-oxide-semiconductor ( $\text{Au}/\text{SnO}_2/\text{n-Si}$ ) MOS structures used in this work were fabricated using n-type (P-doped) single crystals silicon wafer with (111) surface orientation, 300  $\mu\text{m}$  thick. The doping level of silicon wafer was about  $8.33 \times 10^{14} \text{ cm}^{-3}$  showing with the resistivity of about 5  $\Omega\text{-cm}$ . The Si wafer was degreased for 5 min in boiling trichloroethylene, acetone and ethanol consecutively and then etched in a sequence of  $\text{H}_2\text{SO}_4$  an  $\text{H}_2\text{O}_2$ , 20% HF, a solution of  $6\text{HNO}_3:1\text{HF}:35\text{H}_2\text{O}$ , 20%HF. Preceding each cleaning step, the wafer was rinsed thoroughly in deionised water of resistivity of 18 M  $\Omega\text{-cm}$ . Before ohmic contact formed on the n-type Si substrate, the samples were dipped in dilute  $\text{HF}:\text{H}_2\text{O}$  (1:10) about 20 s to remove any native thin oxide layer on the surface, finally the wafer was rinsed by ultrasonic vibration in deionised water. Immediately after surface cleaning, gold (Au, 99.999%) metal with a thickness of 2500 Å for ohmic contacts was thermally evaporated on the back of the wafer in a vacuum-coating unit of  $1 \times 10^{-6}$  Torr. Low-resistance ohmic contacts were formed by thermal annealing at 450 °C for 5 min in flowing  $\text{N}_2$  in a quartz tube furnace and then the wafer was cut into three pieces of about  $5 \times 5 \text{ mm}^2$ . Immediately after ohmic contact, a layer of  $\text{SnO}_2$  was grown on the Si substrate by spraying a solution consisting of 32.21 wt% of ethyl alcohol ( $\text{C}_2\text{H}_5\text{OH}$ ), 40.35 wt% of deionised water ( $\text{H}_2\text{O}$ ) and 27.44 wt% of stannic chloride ( $\text{SnCl}_4 \cdot 5\text{H}_2\text{O}$ ) on the substrate, which was maintained at a constant temperature of 400 °C. The experimental setup used for the films prepared by spray deposition method is described elsewhere [33]. The  $\text{SnO}_2$  films prepared on Si wafer at 5, 10 and 15 s deposition times are denoted by D1, D2 and D3 samples, respectively. The temperature of the substrates was monitored by chromel–alumel thermocouple fixed on top surface of the substrate. The variation of the substrate temperature during spray was maintained within  $\pm 5$  °C with the help of a temperature controller. The rate of spraying was kept at about 30 cc/min. by controlling the carrier gas flow meter.  $\text{N}_2$  was used as the carrier gas.  $\text{SnO}_2$  dots were 3 mm in diameter. After spraying process, circular dots of 1 mm in diameter and 2500 Å thick Au rectifying contacts were deposited onto the  $\text{SnO}_2$  surface of the wafer through a metal shadow mask in liquid nitrogen trapped ultra-high vacuum system in the pressure of  $1 \times 10^{-6}$  Torr. Metal layer thickness as well as deposition rates were monitored with the help of a digital quartz crystal thickness monitor. The deposition rates were about 5–10 Å/s. The thicknesses of  $\text{SnO}_2$  films obtained from the measurement of the oxide capacitance in the strong accumulation region for MOS Schottky diodes were 19, 52 and 191 Å, for D1, D2 and D3 samples, respectively. The capacitance–voltage ( $C$ – $V$ ) and conductance–voltage ( $G$ – $V$ ) measurements were performed at high frequency (500 kHz) by using HP 4192A LF impedance analyzer before and after  $^{60}\text{Co}$   $\gamma$ -ray source irradiation and total dose range was 0–500 kGy at the room

temperature in the dark and test signal of 40 mV<sub>rms</sub>.  $^{60}\text{Co}$  radiation source irradiation with the dose rate 2.12 kGy/h was used for exposing the samples to  $\gamma$ -radiation at room temperature. A set of irradiations were performed changing the exposure time and hence the dose. Changes in their capacitance–voltage ( $C$ – $V$ ) and conductance–voltage ( $G$ – $V$ ) characteristics were measured after each exposure.

### 3. Results and discussion

The dc current voltage measurements preceded the others in order to identify possible leakage through the oxide. As a result, for all the samples used, the leakage current is small. Therefore, the films are proved to be good insulators and the contribution of such currents to the device performance is small.

Fig. 1(a)–(c) depict radiation-induced changes in the measured capacitance as a function of gate voltage before and after  $\gamma$ -ray irradiation 100, 300 and 500 kGy for D1 (19 Å), D2 (52 Å) D3 (191 Å) Au/SnO<sub>2</sub>/n-Si MOS diodes prepared at different oxide layer thicknesses at 500 kHz at room temperature. The three distinct regimes of accumulation–depletion–inversion before and after  $^{60}\text{Co}$   $\gamma$ -ray irradiation are shown. The observed curves showed a irradiation dispersion in accumulation region. As shown in Fig. 1(a)–(c), the values of the capacitance decrease with increasing oxide layer thickness and also the  $C$ – $V$  curves have a peak for D3 sample before and after irradiation. Such behavior of the capacitance peaks are attributed to particular distribution of surface states between SnO<sub>2</sub>/Si interfaces. Therefore, there may be a capacitance due to interface states in excess to depletion layer capacitance. It is also shown from Fig. 1(c) that the change in the oxide layer thickness and gamma-irradiation has effects on the values and positions of these anomalous peaks. The leakage through the oxide is responsible for the slight decrease of the  $C$ – $V$  curves in accumulation region in Fig. 1(a)–(c). The  $C$ – $V$  characteristics after  $\gamma$ -ray irradiation manifests the presence of the trapping centers [34]. The presence of the capacitance peak in the forward capacitance–voltage plot is investigated by a number of experimental result on metal–oxide–semiconductor (MOS) structures [18–20]. The origin of such a peak has been ascribed to the series resistance by Chattopadhyay and Raychaudhuri [20], and Ho et al. [19] to the interface states effect. The values of the capacitance and conductance depend on a number of parameters such as the thickness and formation of the oxide layer, series resistance and density of interface states. The effect of interface state density can be eliminated when the  $C$ – $V$  and  $G/\omega$ – $V$  curves are measured at sufficiently high frequency ( $f \geq 500$  kHz) [6–9,11], since the charges at the interface states cannot follow an ac signal [11]. In this case, the interface states are in equilibrium with the semiconductor. Furthermore, as seen in Fig. 1(a)–(c), it was found to decrease for D1 and D2 samples while the capacitance increases for D3 sample with increase in irradiation dose. Moreover, we can see that from Fig. 1(a) and

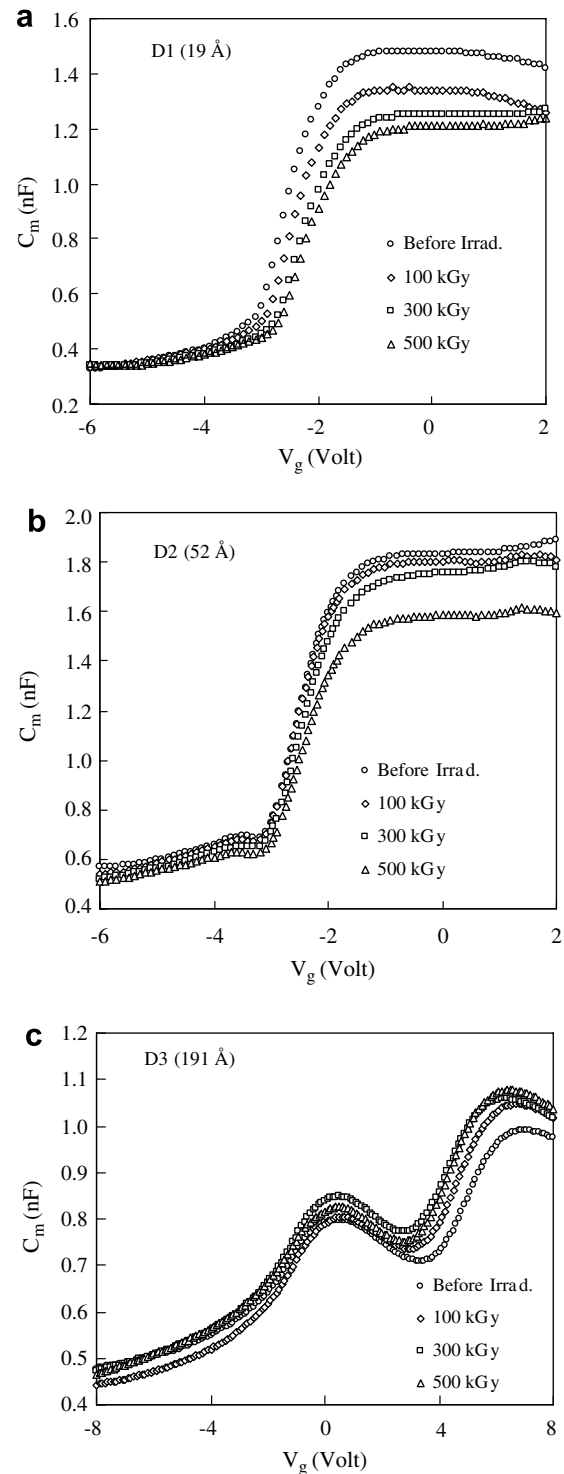


Fig. 1. The measured capacitance ( $C$ ) characteristics versus gate bias ( $V$ ) at 500 kHz at room temperature for (a) D1 (19 Å), (b) D2 (52 Å) and (c) D3 (191 Å) samples prepared at different oxide (SnO<sub>2</sub>) layer thicknesses by spray deposition method before and after different irradiation doses.

(c) while the capacitance values of D1 (19 Å) sample calculated at zero bias in the irradiation range from 0 kGy to 500 kGy varies between 1.48 nF and 1.21 nF, varies between 0.97 nF and 1.05 nF at 8V for D3 (191 Å) sample.

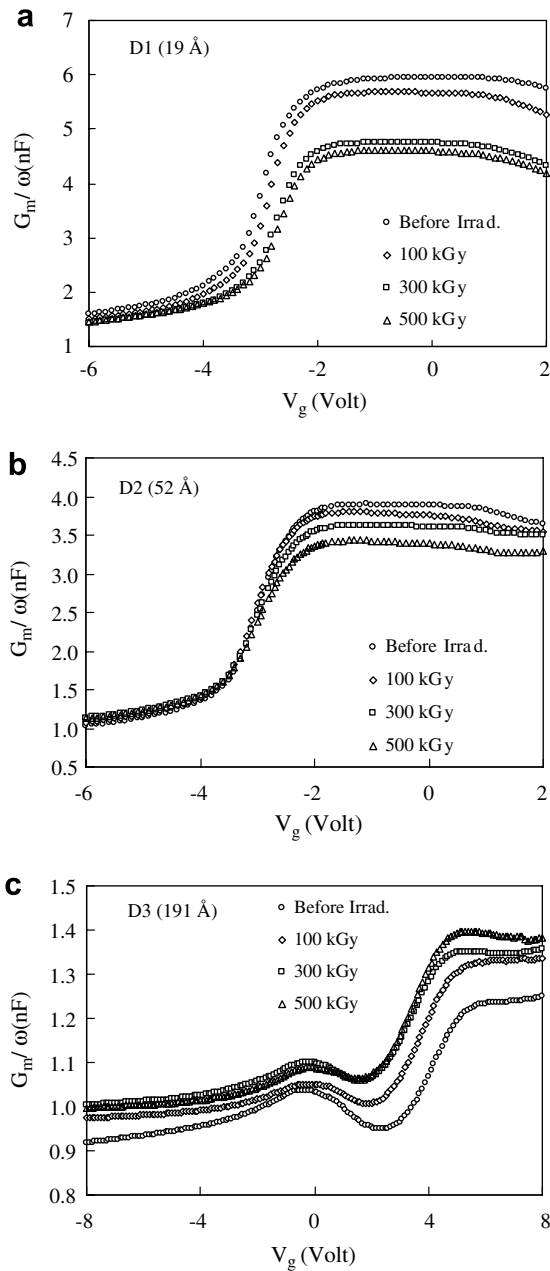


Fig. 2. The measured conductance ( $G/\omega$ ) characteristics versus gate bias ( $V$ ) at 500 kHz at room temperature for (a) D1 (19 Å), (b) D2 (52 Å) and (c) D3 (191 Å) samples prepared at different oxide ( $\text{SnO}_2$ ) layer thicknesses by spray deposition method before and after different irradiation doses.

Fig. 2(a)–(c) show radiation-induced changes in the measured conductance as a function of gate voltage before and after  $\gamma$ -ray irradiation 100, 300 and 500 kGy for all samples prepared at different oxide layer thicknesses at 500 kHz at room temperature. As shown in Fig. 2(a)–(c), the observed curves showed a radiation dispersion in strong accumulation region for D1 and D2 samples and in three distinct regimes for D3 sample. On the other hand, the irradiation dispersion increases with increasing oxide layer thickness.

From the above discussion the series resistance ( $R_s$ ) seems the most important parameter which causes the elec-

trical characteristics of MOS structures to be non-ideal [5,14,20]. The real series resistance of metal-oxide-semiconductor (MOS) Schottky diodes can be determined from the measured capacitance ( $C_{ma}$ ) and conductance ( $G_{ma}$ ) in strong accumulation region at high frequency ( $500 \text{ kHz} \leq f$ ) [14–20]. From  $C$ – $V$  and  $G/\omega$ – $V$  measurements in accumulation, the series resistance  $R_s$  was calculated [14] through relation:

$$R_s = \frac{G_{m,acc}}{G_{m,acc}^2 + (\omega C_{m,acc})^2}, \quad (1)$$

where  $C_{m,acc}$  and  $G_{m,acc}$  are the measured capacitance and conductance in strong accumulation. The series resistance  $R_s$  is an important parameter to designate the noise ratio of device as dependent on irradiation dose. Fig. 3(a)–(c) show the voltage dependence of the series resistance  $R_s$  was calculated from Eq. (1) as a function of gate voltage before and after  $^{60}\text{Co}$   $\gamma$ -ray irradiation 100, 300 and 500 kGy for all samples. The use of the mathematical expressions of the MOS model leads to a series resistance dependent on voltage. As seen in Fig. 3, the series resistance  $R_s$  consists of two parts: One part is independent of  $V$ , the other part decays exponentially with  $V$ . This voltage dependence of  $R_s$  is the result of voltage dependent charges such as interface trapped charge, fixed oxide charge, oxide trapped charge and mobile oxide charge and also at the grain boundaries of  $\text{SnO}_2/\text{Si}$  structures. As seen in Fig. 3, it was found to increase for D1 and D2 samples while the series resistance decreases for D3 sample with increase in irradiation dose.

It is clearly seen in Fig. 3(a)–(c) that the series resistance is virtually independent of voltage at positive voltage for D1 and D2 samples and gives a peak for D3 sample. This peak for D3 sample varies from 3.3 V to 2.5 V before and after different irradiation doses. The peak positions shifted towards lower voltages with increasing irradiation dose, while the magnitude of peak decreases. It is seen from Fig. 3(a)–(c) that the values of the series resistance increase with increasing oxide layer thickness. The series resistance values of  $\text{Au}/\text{SnO}_2/\text{n-Si}$  MOS structure calculated at strong accumulation region at high frequency (500 kHz) and varied to be about 50.4, 66 and 157  $\Omega$  for D1, D2 and D3 samples before irradiation, respectively, and plotted as a function of irradiation dose in Fig. 4. These  $R_s$  values are used to correct the measured  $C$ – $V$  and  $G/\omega$ – $V$  curves. It has been seen that the values of the series resistance  $R_s$  of sample D1 from Fig. 4 varies as 50.4, 53.3, 63.1 and 65.1  $\Omega$  at 0, 100, 300 and 500 kGy, respectively and increases with increasing the irradiation dose. As can be seen in Fig. 4, while the series resistance values of the samples D1 and D2 increase with increasing irradiation dose we found to decrease for D3 sample.

The corrected capacitance  $C_c$  and equivalent parallel conductance  $G_c$  for series resistance were evaluated from the relations:



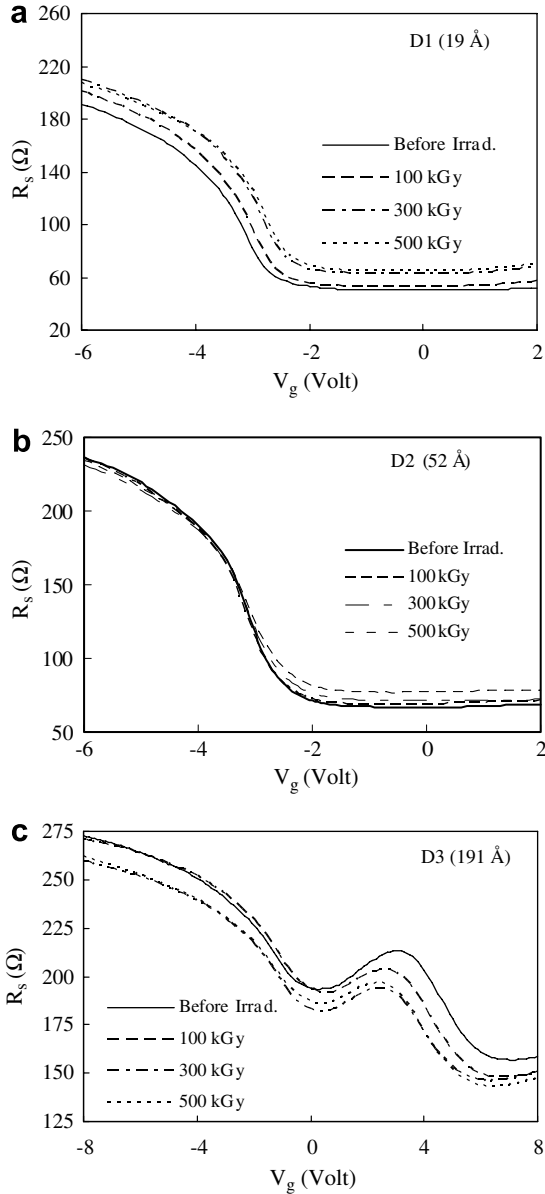


Fig. 3. The gate voltage dependence of the series resistance ( $R_s$ ) at 500 kHz at room temperature for (a) D1 (19 Å), (b) D2 (52 Å) and (c) D3 (191 Å) samples prepared at different oxide ( $\text{SnO}_2$ ) layer thicknesses by spray deposition method before and after different irradiation doses.

$$C_c = \frac{(G_m^2 + \omega^2 C_m^2) C_m}{a^2 + \omega^2 C_m^2}, G_c = \frac{(G_m^2 + \omega^2 C_m^2) a}{a^2 + \omega^2 C_m^2},$$

$$a = G_m - (G_m^2 + \omega^2 C_m^2) R_s \quad (2)$$

where  $C_m$  and  $G_m$  are the measured capacitance and conductance. Fig. 5(a)–(c) depict the voltage dependence of the corrected capacitance  $C_c$  and conductance  $G/\omega$  characteristics for D1, D2 and D3 samples at 500 kHz before irradiation at room temperature. As can be seen from Fig. 5(a)–(c), it is clearly seen that the  $G/\omega$ – $V$  characteristics of D1, D2 and D3 samples consists of a peak. These peaks correspond to the depletion area of the device. The value of interface traps density ( $D_{it}$ ) is determined from this

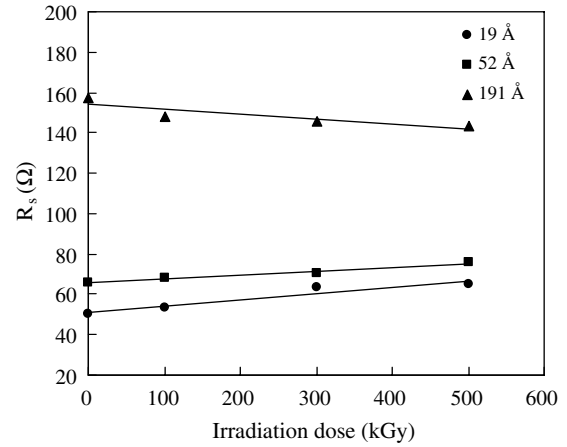


Fig. 4. The series resistance ( $R_s$ ) versus irradiation dose curves of D1 (19 Å), D2 (52 Å) and D3 (191 Å) samples.

peak value. This peak was observed for all samples before and after irradiation dose.

From  $C$ – $V$  and  $G/\omega$ – $V$  measurements in accumulation region, the oxide capacitances  $C_{ox}$  for all samples were calculated [14] through relation:

$$C_{ox} = C_{c,acc} \left[ 1 + \left( \frac{G_{c,acc}}{\omega C_{c,acc}} \right)^2 \right], \quad (3)$$

where  $C_{c,acc}$  and  $G_{c,acc}$  are the corrected capacitance and conductance in accumulation region. The oxide ( $\text{SnO}_2$ ) thickness  $d_{ox}$  calculated from high frequency (500 kHz)  $C$ – $V$  data in strong accumulation using the equation for corrected oxide layer capacitance ( $C_{ox} = \epsilon_i \epsilon_0 A / d_{ox}$ ), where  $\epsilon_i = 7\epsilon_0$  [5,6] and  $\epsilon_0$  are the permittivity of the interfacial insulator layer and free space, has been determined to be about 19, 52 and 191 Å, for D1, D2 and D3 samples, respectively.

Measurement of the density of interface states ( $D_{it}$ ) at the  $\text{SnO}_2/\text{n-Si}$  interface is a useful guide to the quality of the MOS diodes. A number of different methods have been used to measure  $D_{it}$  from the capacitive and conductive response of the interface states to a small external ac signal. An excellent analysis on the subject can be found in handbook [14]. The application of a single-frequency approximation method [21] allows estimation of the density of interface states from the  $G$ – $V$  measurements. A fast and reliable way to determine the density of interface states ( $D_{it}$ ) is the Hill-Coleman method [21] and confirmed by Konofaos [22] and Dakhel [23]. According to this method,  $D_{it}$  can be calculated using the following formula:

$$D_{it} = \frac{2}{qA} \frac{G_{c,max}/\omega}{[(G_{c,max}/\omega C_{ox})^2 + (1 - C_c/C_{ox})^2]}, \quad (4)$$

where  $A$  is the area of the diode,  $\omega$  is the angular frequency,  $q$  is the elementary electrical charge,  $C_{ox}$  is the capacitance of oxide layer in accumulation region of  $C_c$ – $V$  curves,  $G_{c,max}$  conforms to maximum corrected  $G$ – $V$  curve;  $C_c$  is capacitance of the diodes corresponding to  $G_{c,max}$ . This method was applied on  $G$ – $V$  curves of the

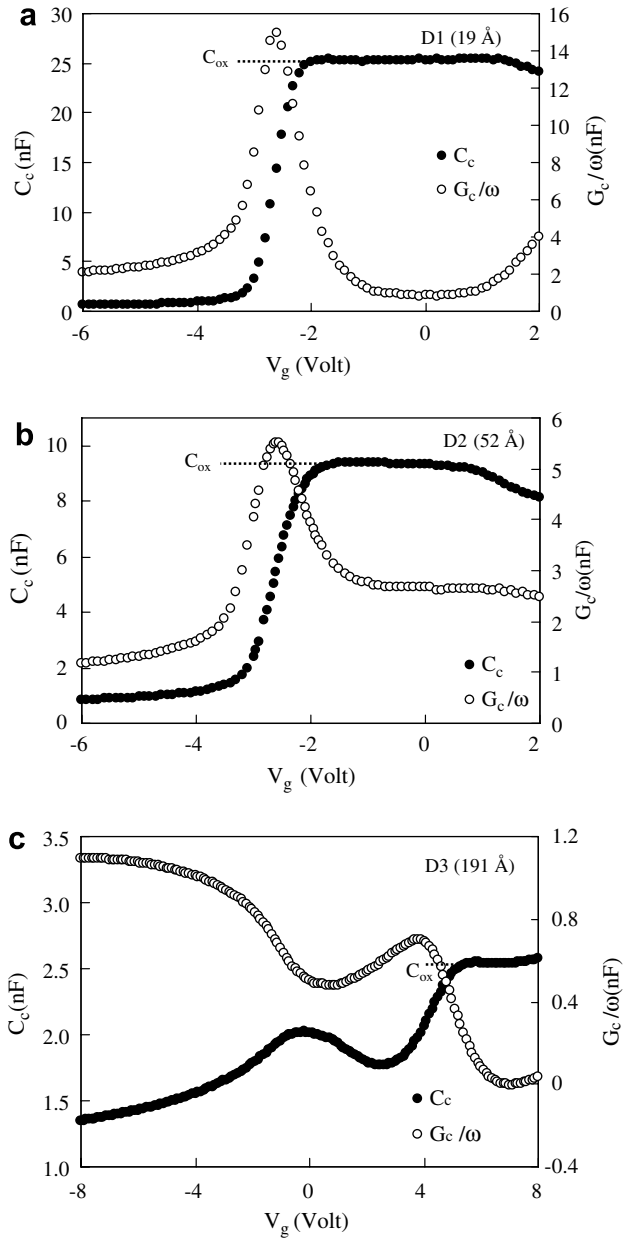


Fig. 5. The voltage dependent plots of the corrected capacitance ( $C$ ) and corrected conductance ( $G/\omega$ ) for (a) D1 (19 Å), (b) D2 (52 Å) and (c) D3 (191 Å) samples at room temperature at 500 kHz before irradiation.

frequency of 500 kHz. The curve shown is for the as-measured data with the effects of series resistance being corrected for and this is the one used for the  $D_{it}$  calculation via the Hill-Coleman equation. The peaks corresponds to the depletion area of the device and its existence verifies the presence of interface traps [11,31,32]. Similar behavior were obtained for all samples, verifying the MOS behavior with interface states. This method is very useful in understanding the electrical quality of the interface and the obtained values of the interface traps are shown as a function of irradiation dose in Fig. 6. As can be seen from Fig. 6, while the interface trap density value of the samples D1 and D2 decrease with increasing irradiation dose we

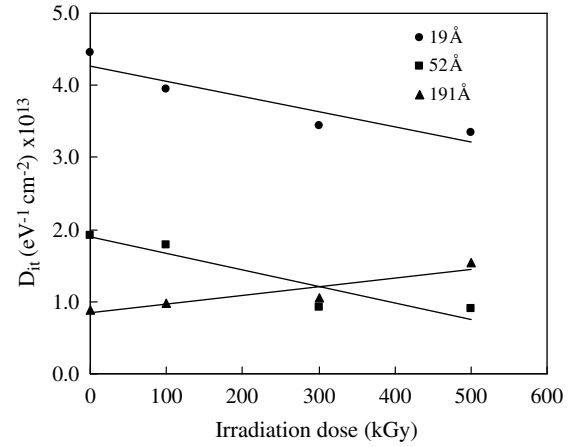


Fig. 6. The interface trap density ( $D_{it}$ ) versus irradiation dose curves of D1 (19 Å), D2 (52 Å) and D3 (191 Å) samples.

found to increase for D3 sample. On the other hand, for D1 and D2 samples, it is seen that the interface traps passivate while the irradiation dose increases.

Especially there are two important effects of radiation to be considered: (a) the transient effects due to the electron–hole pair generation and (b) permanent effect due to the bombardment of devices with radiation, causing changes in the crystal lattice. The radiation-generated holes may diffuse in the oxide, but are less mobile than the electrons; many stationary holes traps are also present. The radiation-induced damage is also directly related to the amount of energy absorbed by the device material or the total dose of radiation received by the device. Our experimental results depict an increase in the change in capacitance and conductance due to the radiation-induced defects at the interface and decrease in the interface states  $D_{it}$  with increasing radiation dose for D1 (19 Å) and D2 (52 Å) samples. Such a behavior of  $D_{it}$  is attributed to the existence of an interfacial oxide layer between the metal and semiconductor that passivates the surface of semiconductor. On the other hand, the density of interface states  $D_{it}$  decreases with increasing radiation dose, being attributed to the decrease in the recombination centers. Furthermore, as seen in Fig. 6, the radiation-induced damage in the interface is permanent for D3 (191 Å) sample since the number of interface traps increases with irradiation dose.

It has been seen that the interface state density ( $D_{it}$ ) values of sample D1 from Fig. 6 vary as  $4.45 \times 10^{13}$ ,  $3.94 \times 10^{13}$ ,  $3.43 \times 10^{13}$  and  $3.35 \times 10^{13} \text{ eV}^{-1} \text{ cm}^{-2}$  at 0, 100, 300 and 500 kGy, respectively and decreases with increasing the irradiation dose. Furthermore, interface trap density ( $D_{it}$ ) values of samples D1, D2 and D3 vary as  $4.45 \times 10^{13}$ ,  $1.92 \times 10^{13}$  and  $0.89 \times 10^{13} \text{ eV}^{-1} \text{ cm}^{-2}$  before irradiation, respectively. Moreover, it is seen that the interface traps decrease while the oxide thickness increases. However, the calculated values of  $D_{it}$  ( $\approx 10^{13} \text{ eV}^{-1} \text{ cm}^{-2}$ ) is not high enough to pin the Fermi level of the Si substrate disrupting the device operation [22,23]. Consequently, the interface traps and defects cannot prevent the construction of an MOS device. The values obtained for  $D_{it}$  are of the

same order as those reported by some authors for Schottky diodes [6,20,22,23].

#### 4. Conclusions

We conclude that prepared Au/SnO<sub>2</sub>/n-Si MOS Schottky diodes have been controlled by the insulator layer and interface states, which are responsible for the non-ideal behaviour of  $C-V$  and  $G/\omega-V$  characteristics. The forward and reverse bias capacitance–voltage ( $C-V$ ) and conductance–voltage ( $G/\omega-V$ ) characteristics of Au/SnO<sub>2</sub>/n-Si MOS diodes prepared at three different oxide (SnO<sub>2</sub>) layer thicknesses by spray deposition method were measured at 500 kHz before and after different irradiation doses. Samples were exposed at 100, 300 and 500 kGy. The effects of the series resistance ( $R_s$ ) and interface traps density ( $D_{it}$ ) of Au/SnO<sub>2</sub>/n-Si MOS diodes on  $C-V$  and  $G-V$  characteristics before and after irradiation dose are investigated. It is found that both capacitance and conductance were quite sensitive to irradiation dose and while the capacitance, conductance, and series resistance for D1 and D2 samples decrease with increasing irradiation dose we found to increase for D3 sample. The series resistance values of Au/SnO<sub>2</sub>/n-Si MOS structure calculated at accumulation region at 500 kHz and varied to be about 50.4, 66 and 157  $\Omega$  for D1, D2 and D3 samples, respectively, and increased with increasing oxide layer thickness. The values of the interface state density located in the n-Si band gap at the SnO<sub>2</sub>/n-Si interface prepared in the different oxide layer thicknesses, 0.89, 0.97, 1.06 and  $1.53 \times 10^{13} \text{ eV}^{-1} \text{ cm}^{-2}$  for sample D3 at 0, 100, 300 and 500 kGy, respectively, has been determined. It is found that the calculated values of  $D_{it}$  ( $\approx 10^{13} \text{ eV}^{-1} \text{ cm}^{-2}$ ) is not high enough to pin the Fermi level of the Si substrate disrupting the device operation and also the density of interface states for Au/SnO<sub>2</sub>/n-Si diodes is high when compared to insulators such as SiO<sub>2</sub>.

#### References

- [1] J.L. Brousseau, H. Bourque, A. Tessier, R.M. Leblanc, Appl. Surf. Sci. 108 (1997) 351.
- [2] M. Mwamburi, E. Wäckelgård, A. Roosb, Thin Solid Films 374 (2000) 1.
- [3] R.K. Sharma, P.C.H. Chan, Z. Tang, G. Yan, I.M. Hsing, J.K.O. Sin, Sens. Actuat. B 72 (2001) 160.
- [4] H. Yan, G.H. Chen, W.K. Man, S.P. Wong, R.W.M. Kwok, Thin Solid Films 326 (1998) 88.
- [5] S. Karadeniz, N. Tuğluoğlu, T. Serin, Appl. Surf. Sci. 233 (2004) 5.
- [6] S. Karadeniz, N. Tuğluoğlu, T. Serin, N. Serin, Appl. Surf. Sci. 246 (2005) 30.
- [7] D. Nisiro, G. Fabbri, G.C. Celotti, A. Bellosi, J. Mater. Sci. 38 (2003) 2727.
- [8] M. Mehdi Bageri-Mohagheghi, M. Shokooh-Saremi, Semicond. Sci. Technol. 19 (2004) 764.
- [9] R. Ayouchi, F. Martin, J.R. Ramos Barrado, M. Martos, J. Morales, L. Sánchez, J. Power Sources 87 (2000) 106.
- [10] F.M. Amanullah, M. Saleh Al-Mobarak, A.M. Al-Dhafiri, K.M. Al-Shibani, Mater. Chem. Phys. 59 (1999) 247.
- [11] V. Bilgin, S. Köse, F. Atay, İ. Akyüz, Mater. Lett. 58 (2004) 3686.
- [12] U.R. Chaudhuri, K. Ramkumar, M. Satyam, J. Phys. D: Appl. Phys. 23 (1990) 994.
- [13] E.H. Rhoderick, R.H. Williams, Metal-Semiconductor Contacts, Oxford Press, Clarendon, 1988.
- [14] E.H. Nicollian, J.R. Brews, MOS Physics and Technology, Wiley, New York, 1982.
- [15] E.H. Nicollian, A. Goetzberger, Appl. Phys. Lett. 7 (1965) 216.
- [16] A. Singh, Solid-State Electron. 28 (1985) 233.
- [17] E.H. Nicollian, A. Goetzberger, Bell. Syst. Technol. J. 46 (1967) 1055.
- [18] P. Chattopadhyay, A.N. Daw, Solid State Electron. 29 (5) (1986) 555.
- [19] P.S. Ho, E.S. Yang, H.L. Evans, Xu Wu, Phys. Rev. Lett. 56 (1986) 177.
- [20] P. Chattopadhyay, B. Raychaudhuri, Solid-State Electron. 35 (1992) 875; P. Chattopadhyay, B. Raychaudhuri, Solid-State Electron. 35 (1992) 1023; P. Chattopadhyay, B. Raychaudhuri, Solid-State Electron. 36 (1993) 605.
- [21] W.A. Hill, C.C. Coleman, Solid State Electron. 23 (1980) 987.
- [22] N. Konofaos, Microelectron. J. 35 (2004) 421.
- [23] A.A. Dakhel, Thin Solid Films 496 (2006) 353.
- [24] O.I. Shpotyuk, Radiat. Phys. Chem. 46 (1995) 1279.
- [25] V. Mucka, J. Podlaha, R. Silber, Radiat. Phys. Chem. 59 (2000) 467.
- [26] E. Atanassova, A. Paskaleva, R. Konakova, D. Spassov, V.F. Mitin, Microelectron. J. 32 (2001) 553.
- [27] J.D. Zhang, S. Fung, L. Li-Bin, L. Zhi-Jun, Surf. Coat. Technol. 158/159 (2002) 238.
- [28] K. Arshak, O. Korostynska, J. Haris, Proc. MIEL 1 (2002) 357.
- [29] K. Arshak, O. Korostynska, Sensor Rev. 23 (2003) 48; K. Arshak, O. Korostynska, Sens. Actuat. A 113 (2004) 307; K. Arshak, O. Korostynska, Sens. Actuat. A 113 (2004) 319.
- [30] R.y. Zhu, Nucl. Instr. and Meth. A 413 (1998) 297.
- [31] L.N. Trefilova, A.M. Kudin, L.V. Kovaleva, T.A. Charkina, A.I. Mitichkin, L.E. Belenko, Radiat. Meas. 33 (2001) 687.
- [32] G. Pacchioni, Solid State Sci. 2 (2000) 161.
- [33] T. Serin, N. Serin, S. Karadeniz, H. Sari, N. Tuğluoğlu, O. Pakma, J. Non-Cryst. Solids 352 (2006) 209.
- [34] M. Walters, A. Reisman, J. Appl. Phys. 67 (1990) 2992.